RETRIEVAL OF LUNAR SURFACE TEMPERATURE AND SPECTRAL EMISSIVITY IN 3-5 μm RANGE FROM CHANDRAYAAN-2 IIRS OBSERVATIONS. Satya Prakash Ojha[1], Vikram KVNG[1] and Satadru Bhattacharya[1], [1]Planetary Science Division, Biological and Planetary Sciences and Applications Group, Space Applications Centre, Ahmedabad-380058, India. satyap@sac.isro.gov.in.

Introduction: The Moon's surface thermal environment is among the most extreme of any planetary body in the solar system [1]. The surface temperature of the Moon governs the thermal state of the Moon's regolith and interior, and the behavior of near-surface volatiles [2]. Highly accurate surface temperatures at local times are required for the development of thermo-physical models of the lunar regolith. It is also needed for the thermal correction of the surface reflectance measurements which can improve the accuracy of lunar surface composition mapping. The brightness temperature (BT) is lower than the physical temperature due to the non-unity emissivity for most surfaces and has significant spatial variation. Here we present initial results of the simultaneous retrieval of lunar surface temperature and surface spectral emissivity in 3-5 μm range, from Chandrayaan-2 Imaging Infrared Spectrometer (IIRS, [3]) observations.

Retrieval algorithm: The simultaneous retrieval of lunar surface temperature and spectral emissivity is performed using optimal estimation [4]. Given a set of radiance (or equivalent BT) observations **y** and a priori state vector $\mathbf{x}^a$ representing the system state at the observation location, we seek an optimal state **x** that minimizes the distance between the model *a priori* state and the observed radiances. When the model *a priori* and observation errors are uncorrelated and have a Gaussian distribution, then the optimal estimate of the state vector **x** is the minima of the following cost function $J(\mathbf{x})$:

$$J(\mathbf{x}) = (\mathbf{x}-\mathbf{x}^a)^T\mathbf{S}_a^{-1}(\mathbf{x}-\mathbf{x}^a) + (\mathbf{y}-F(\mathbf{x}))^T\mathbf{S}_\mathbf{y}^{-1}\big(\mathbf{y}-F(\mathbf{x})\big) \quad (1)$$

where F is the forward model simulating the observed radiance (or equivalent BT) **y** given the model state **x**. $\mathbf{S}_a$ and $\mathbf{S}_y$ are the *a priori* and observation error covariance matrices respectively. The $\mathbf{S}_a$ and $\mathbf{S}_y$ are considered to be diagonal. The forward model F used here is given as

$$I_\lambda = (1-\epsilon_\lambda)\frac{J_\lambda \cos(\theta)}{\pi d^2 \cos(e)} + \epsilon_\lambda \frac{2hc^2}{\lambda^5}\frac{1}{e^{\frac{hc}{\lambda k T_s}}-1} \quad (2)$$

where I_λ is the spectral radiance measured by IIRS at wavelength λ, h is the Planck's constant, c is the speed of light, k is the Boltzmann constant. J_λ is the spectral solar irradiance at wavelength, d is the mean Sun-Moon distance in astronomical units, θ is the incidence angle, and e is the emergence angle.

In Eq. 2, spectral emissivity ϵ_λ and the surface temperature T_s are unknown variables and I_λ is the known variable. The surface temperature remains unchanged with wavelength. Hence, N channel observations correspond to N + 1 unknowns (N emissivity and 1 surface temperature). The number of unknowns is larger than that of equations. If we have another set of observations available at the same location at different time instant then there will be 2N observations and N + 2 unknowns (N emissivity and 2 surface temperatures, assuming emissivity time invariant) and the system can be solved. It is possible only if we have repetitive observations at the same location. In case of IIRS, obtaining repetitive observations is difficult. To create another set of observations we took the average of the eight nearby neighboring pixels. Emissivity is assumed to be same in the 3 × 3 box. With this assumption, the T_s will be retrieved at the pixel resolution however emissivity will be retrieved at every third pixel. Accordingly, the state vector for optimal estimation is defined as $\mathbf{x} = (\epsilon_{\lambda_1}, \epsilon_{\lambda_2}, \dots, \epsilon_{\lambda_m}, T_s, \overline{T}_s)^T$ and the observation vector as $\mathbf{y} = (I_{\lambda_1}, I_{\lambda_2}, \dots, I_{\lambda_m}, \bar{I}_{\lambda_1}, \bar{I}_{\lambda_2}, \dots, \bar{I}_{\lambda_m})^T$. T_s represents the surface temperature of the center pixel while $\overline{T}_s$ corresponds to the average temperature of surrounding 8 pixels. Similarly, I_{λ_i} represents the radiance observations at the center pixel and $\bar{I}_{\lambda_i}$ denotes the average radiance observations of the surrounding 8 pixels.

For the physical retrieval of lunar surface temperature and surface spectral emissivity we used IIRS observations in the range of 3-5 μm. The observations are affected by the order sorting filters (OSF), so those channels are avoided where OSFs are placed. Few other channels, in the immediate vicinity of the OSFs, are also rejected as their quality was not found to be good for retrieval. A total of 69 channels are used for the retrieval. The *a priori* surface temperature, T_s^a, is calculated by inverting the Planck's function

$$T_s^a = \frac{hc}{\lambda k \log\left(\frac{2hc^2\epsilon_\lambda}{\lambda^5 I_\lambda}+1\right)} \quad (3)$$

I_λ is the radiance observation at $\lambda = 4.8749\ \mu m$. The emissivity value $\epsilon_{\lambda=4.8749\ \mu m}$ is taken as 0.85.

The *a priori* emissivity, ϵ_λ^a, is calculated from Eq. 2 by using the T_s^a, values, calculated as described above. The *a priori* emissivity values are calculated for all selected wavelengths (λ_i) at each pixel. The averaged values of ϵ_λ^a in 5 × 5 box, excluding the inner 3 × 3 box, are used as *a priori* emissivity. Again, here the *a priori* is prepared in this manner in order to avoid the correlation between the observations and the *a priori*.

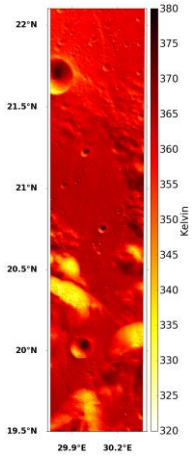

Figure 1 Retrieved surface temperature

Results and discussion: The spatial plot of the retrieved surface temperature is shown in Figure 1. The surface temperature ranges from 320-380 K. This range agrees well with the reported temperatures over lunar surface by various authors [5,6].

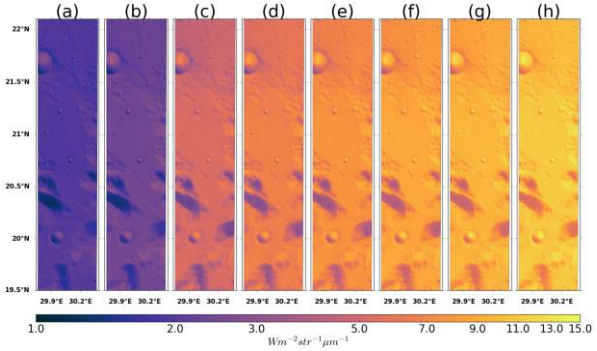

Figure 2 Radiance plots for (a) λ= 3.0717 μm, (b) λ= 3.2233 μm, (c) λ= 3.9817 μm (d) λ= 4.1671 μm, (e) λ= 4.3524 μm, (f) λ= 4.5210 μm, (g) λ= 4.7063 μm, (h) λ= 4.8580 μm.

The spatial plots of the IIRS radiance and retrieved emissivity at few selected wavelengths are shown in Figures 2 and 3 respectively. The emissivity plots show significant spatial variation for small wavelengths. For large wavelengths the spatial variation is quite low. The forward model uses Kirchoff's law which is valid if the surface is isothermal in the infrared skin depth. In the presence of strong thermal gradients, the Kirchoff's law is not valid. As minerals become more transparent (for example at frequencies higher than about 1400 cm^{-1} or wavelengths shorter than 7 μm for silicates), spectral behavior becomes dominated by volume scattering at all particle sizes. However, laboratory measurements of spectral emittance indicate that Kirchoff's law is still qualitatively valid. This becomes extremely complex in the transition region [7]. Radiative transfer models such as Hapke [8], includes the multiple scattering effects of the upwelling thermal emission which may be a more accurate representation of the potential thermal effects compared with models solely based on Kirchoff's law. The retrieval of surface temperature and emissivity with Hapke model, using IIRS observations, will be explored in future work.

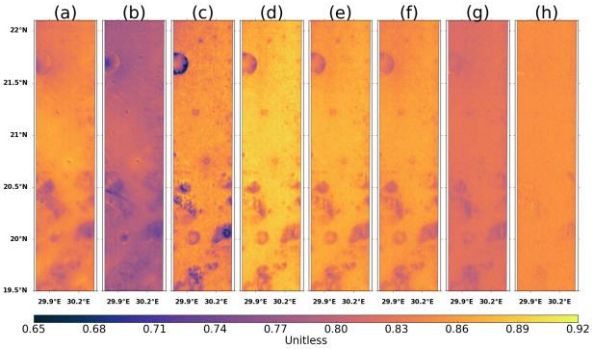

Figure 3 Spatial plots of the retrieved surface emissivity plots for wavelengths mentioned in Fig. 2.

Acknowledgments: The authors would like to thank Shri Nilesh Desai, Director SAC, Dr. I. M. Bahuguna, DD, EPSA/SAC, Dr. Bimal Kumar Bhattacharya, GD, BPSG/EPSA/SAC and Dr. A. S. Arya, Head, PSD/BPSG/EPSA/SAC for their guidance. We thank Shri Aditya Dagar, Scientist, PSD/BPSG/EPSA/SAC for his help during the course of this work. The Chandrayaan-2 IIRS data is obtained from https://pradan.issdc.gov.in.

References:

[1] D. A. Paige et al. (2010a), Science, 330, 479-482. [2] D. A. Paige et al. (2010b), Space Sci. Rev., 150, 125-160. [3] Chowdhury, et al. (2020), Current Sci., 118(3), 368–375. [4] Maahn et al. (2020) BAMS, 101 (9), E1512-E1523. [5] Williams et al. (2017), Icarus, 283, 300-325. [6] Hu et al. (2016), IEEE GRSL, 13(1), 110-114. [7] Salisbury, et al., 1987 USGS report [8] B. Hapke (1981), JGR, 86, 3039-3054.